Characterization of NBR Networks from Stress–Strain and Swelling Equilibrium Measurements*

A. M. HASSAN and L. N. RAY, JR., *Research and Development Center, Armstrong Cork Company, Lancaster, Pennsylvania 17604*

Synopsis

An improved stress–strain (S/S) method based on rubber elasticity theory and swelling equilibrium measurements was used to investigate the S/S behavior and the solvent swelling properties of nitrile–butadiene rubber (NBR) and also to study the effects of varying the cure agent and the curing conditions on the crosslinking efficiency in NBR vulcanizates. The S/S curve of completely swollen NBR vulcanizates is, as expected, in agreement with rubber elasticity theory, while that of dry or partially swollen vulcanizates is well described by the Mooney-Rivlin equation. Determined in benzene, χ was 0.494, compared to 1.338 in cyclohexane and 2.124 in n-heptane. The degree of crosslinking and the crosslinking efficiency in the NBR vulcanizates, moles of crosslinks produced per mole of crosslinking agent employed in the formula, are largely dependent on the nature of the crosslinking agent used and increase in the following order: peroxide, sulfur tetramethylthiuram disulfide, sulfur N-cyclohexyl-2-benzothiazolesulfenamide, sulfur benzothiazyl disulfide, and finally tetramethylthiuram disulfide.

INTRODUCTION

The elementary form of the rubber elasticity theory (RET) derived for a Gaussian distribution of the chains in a polymeric network defines the stress f/A_0 in vulcanized dry rubber in terms of the extension ratio α by the simple relationship[1]

$$f/A_0 = \nu kT(\alpha - \alpha^{-2}) = \rho RT(M_c)^{-1}(\alpha - \alpha^{-2}) \tag{1}$$

where f is the force; A_0 is the cross-sectional area of the unstrained sample; T is the absolute temperature; k is the Boltzmann constant; ν is the number of elastically active network chains per unit volume; and M_c is the molecular weight between the crosslinks. The observed stress–strain, however, shows a significant departure from the theoretical results given in eq. (1), and in most cases the stress–strain curve in simple extensions is better described by the Mooney-Rivlin equations[2,3]:

$$\phi = (f/2A_0)v_r^{1/3}(\alpha - \alpha^{-2})^{-1} = C_1 + C_2\alpha^{-1} \tag{2}$$

where v_r is the volume fraction of rubber in the swollen sample and C_1 and C_2 are constants. A plot of ϕ versus α^{-1} should give a straight line with an

---

* Presented in part at American Chemical Society Third Middle Atlantic Regional Meeting, February 1–2, 1968, Philadelphia, Pennsylvania.

intercept of C_1 and a slope of C_2.   The intercept C_1 has been identified with the RET function of eq. (1) to give

$$C_1 = \frac{1}{2}\nu kT = \frac{1}{2}\rho RT(M_c)^{-1} \tag{3}$$

while C_2, of unknown molecular origin, accounts for the departure of the S/S curve from the RET eq. (1).

As we shall show later, ϕ is sensitive to errors in α.   This sensitivity is extremely large in the low extension region for $\alpha = 1.0$ to 1.3 and relatively small in the high extension regions.   An error in α should affect the various parts of the ϕ-versus-α^{-1} plot differently, leading to a significant departure from the expected linearity, especially in the low extension region.   This departure affects the slope of the curve, C_2, and, more significantly, introduces an error in C_1 which is the parameter employed in calculating M_c and ν.   An improved method for evaluating α and therefore ϕ is proposed. The method which allows for a good evaluation of C_2 and C_1 and M_c from the S/S experiment was employed in conjunction with the swelling equilibrium measurements: (1) to investigate the S/S and the solvent swelling properties of a series of rubber networks, (2) to calculate their polymer interaction parameter χ, and (3) to evaluate, quantitatively, the effects of varying the cure agent and cure conditions on crosslinking efficiency in these networks.   Characterization of a nitrile–butadiene rubber (NBR) network by these methods is described in the present paper while characterization of ethylene–propylene rubber and ethylene–propylene terpolymer networks by the same methods is described in a separate paper.[4]

EXPERIMENTAL

NBR Vulcanizates

The various NBR vulcanizates examined are shown in Table I.   The vulcanizates were prepared from a commercial acrylonitrile–butadiene copolymer (32% to 34% acrylonitrile) in the presence of (1) dicumyl peroxide, (2) sulfur accelerated with benzothiazyl disulfide (Altax), N-cyclohexyl-2-benzothiazolesulfenamide (Santocure), or tetramethylthiuram disulfide (Methyltuads), and (3) Methyltuads alone.   Concentrations of cure agent and coagent as well as cure time were varied to produce a wide range of crosslinked networks.   Cure temperature, however, was held at 158°C. The vulcanizates were prepared by press molding to give a 0.2-cm thickness sheet from which a dumbbell shape sample were cut using a standard 1.5-in. die (ASTM D 599-61).

Experimental Method

All stress–strain measurements were made at 25°C and extension rates were 1.37 cm/min using the apparatus shown in Figure 1, which was constructed in our laboratory.   The sample was extended 0.2 cm per extension and then held under load for 12 min while maintaining it at fixed elongation.   The force was read from the recorded force–time curve, and the

TABLE I
Composition[a] of NBR Vulcanizates

Cure agent	Nitrile rubber	ZnO	Stearic acid	Sulfur	Thiazole[b] accelerator	Sulfenamide[c] accelerator	Thiuram[d] accelerator	Dicumyl peroxide
1. Peroxide	100	—	—	—	—	—	—	1 to 4
2. Sulfur	100	5	1	2	0.5 to 3	—	—	—
	100	5	1	2	—	0.5 to 2	—	—
	100	5	1	2	—	—	0.5 to 2	—
3. Thiuram	100	5	1	—	—	—	1 to 4	—

[a] phr.
[b] Benzothiazyl disulfide (Altax).
[c] N-Cyclohexyl-2-benzothiazolesulfenamide (Santocure).
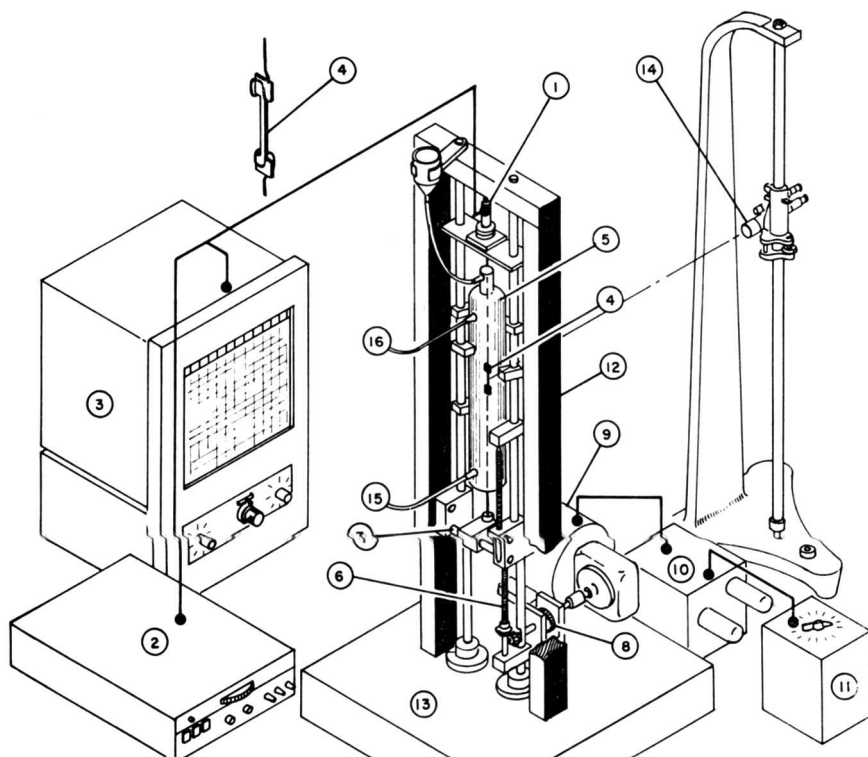[d] Tetramethylthiuram disulfide (Methyltuads).

Fig. 1. Stress–strain apparatus: ① strain gage; ② dc power supply; ③ recorder; ④ sample; ⑤ swelling cell; ⑥ jack screw; ⑦ sliding cross bar; ⑧ reduction gear ratio 4:1; ⑨ dc motor, 10–173 rpm; ⑩ motor controller; ⑪ current input controller; ⑫ metal frame; ⑬ wooden base; ⑭ cathetometer; ⑮ from pump (reservoir); ⑯ to reservoir.

length was measured to ±0.001 cm by a cathetometer between two marks made on the sample by introducing two thin wires about 3.5 cm apart in the narrow region of the sample. When the stress–strain measurement was made on swollen vulcanizates, the swelling was made directly in the swelling cell, Figure 1, using benzene. In order to establish swelling equilibrium conditions, it was necessary to leave the sample in benzene or benzene atmosphere overnight in the tightly sealed glass swelling cell. Assuming an isometric volume expansion of the rubber sample during swelling, the volume fraction of the rubber in the swollen sample, v_r, was calculated from

$$v_r = [L_0(\text{dry})/L_0(\text{swollen})]^3 \tag{4}$$

where L_0 (dry) and L_0 (swollen) obtained from f-versus-L^{-1} plot are the initial lengths of the sample before and after swelling, respectively. This method of evaluating v_r leaves the sample undisturbed and was found to be in agreement with v_r established from gravimetric measurements.

RESULTS AND DISCUSSION

Characterization of rubber networks can be made from stress–strain measurements through the use of rubber elasticity theory and from swelling equilibrium measurements using the Flory-Rehner equation. The use of the second method, which is simple to perform, is contingent on the knowledge of the solvent–polymer interaction parameter χ. In this investigation, both methods were employed: stress–strain measurements were performed first followed by swelling equilibrium and χ determination.

Data Treatment

The stress–strain behavior of rubber networks can be described by the use of the simple RET eq. (1) or its modified form, eq. (2). Dry rubber networks exhibit a S/S curve which deviates considerably from the ideal condition described by eq. (1), and their S/S is better described by eq. (2).

The function $(\alpha - \alpha^{-2})^{-1}$ of eq. (2) is plotted versus α^{-1} in Figure 2, which also shows a S/S plot of $f/2A_0$ versus α (curve 2) and ϕ versus α^{-1} (curve 3) for a lightly crosslinked rubber network. If we draw a vertical line passing through the three curves, then, according to eq. (2), the point of intersection on curve 3, ϕ, is equal to $(\alpha - \alpha^{-2})^{-1}$, the intersection point on curve 1, times $f/2A_0$, the intersection point on curve 2. Thus, one way of generating curve 3 is to multiply every $(\alpha - \alpha^{-2})^{-1}$ point on curve 1 by the $f/2A_0$ value on curve 2, both points taken at the same α value and then plot the product versus the inverse of that α value. Below $\alpha \leq 0.8$, the ϕ values are seen to fall on a straight line, but they deviate considerably from this line in the low extension region, $\alpha^{-1} \geq 0.8$. Examination of Figure 2 shows that errors in measuring $f/2A_0$ are not expected to account for
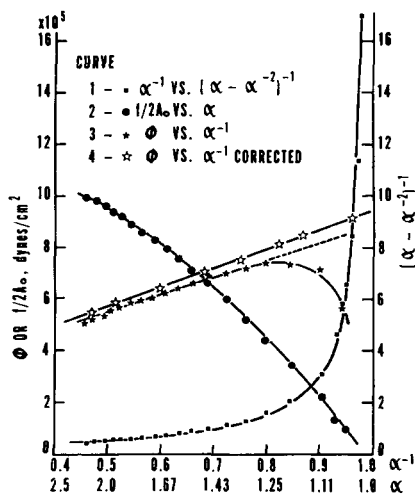

Fig. 2. Stress–strain in NBR vulcanizates. Curve 4 was established by correcting α values used in curve 3 by a small fraction, e.g., in the low extension region this correction amounts to about -1.8% α.

this drastic deviation. For example, a 2% error in measuring $f/2A_0$, which is considerably larger than the real errors in measuring this parameter, should lead only to 2% error in ϕ. Much larger errors in estimating ϕ, however, are expected to arise when small errors are made in estimating α, especially in the region $\alpha^{-1} \geq 0.8$. This is due to the large sensitivity of $(\alpha - \alpha^{-2})^{-1}$ to changes in α. As shown in curve 2, Figure 2, the $(\alpha -$
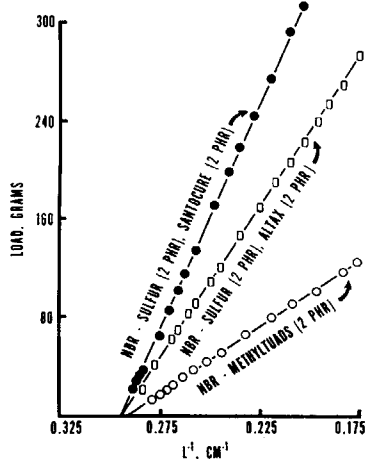

Fig. 3. Load vs. elongation^{-1} in NBR vulcanizates.

$\alpha^{-2})^{-1}$ function exhibit a sharp rise, asymptotic, in the low extension region, and hence small errors in α in this region should lead to serious errors in estimating ϕ. To illustrate if the α values used to compute curve 3 in Figure 2 are modified by -1.8% (corresponding to a -1.8% error in α), the ϕ-versus-α^{-1} plot curve will be as shown by curve 4, Figure 2, in which all the points fall on a straight line.

Errors in estimating $\alpha = L/L_0$ arise either from measuring the elongation L or from estimating the initial length of the sample at zero force, L_0. The first type of error is relatively insignificant. In the present work, L was in the range 3.4–3.6 cm, with errors made in measuring L of the order of ± 0.001 cm. If L_0 is estimated from f-versus-L plots, much larger errors, e.g., up to 3%, may be encountered because of the curvature of f-versus-L plots at low values of f. Errors of this magnitude should lead to large errors in estimating the function $(\alpha - \alpha^{-2})^{-1}$ and consequently in ϕ. This condition suggests that a reliable method for establishing L_0 is needed. The best L_0 values for the present networks were obtained by plotting f-versus-L^{-1} and extrapolating to zero force. Figure 3 shows a series of curves established by the f-versus-L^{-1} method for various NBR vulcanizates. In each case, the experimental data fell on a straight line for extensions, depending on the sample, up to 150%. For the low extension region, this gives a straight line with a unique intercept, and, therefore, establishes a reliable L_0 value.

The effect of errors made in estimating L_0 on ϕ was examined in detail through the use of a computer program which allows for introducing errors in L_0 in the order of $\pm 0.02\%$ or more. The plot of ϕ versus α^{-1} shown in Figure 4 demonstrates some of the results obtained from this treatment for an NBR–peroxide vulcanizate sample. The various curves shown in this figure were obtained by plotting ϕ versus α^{-1} for this sample at various L_0 values. The only straight line in the series, marked L_0, was obtained by using an $L_0 = 3.4867$ cm established from an f-versus-L^{-1} plot. The remaining curves were established by using an $L = 3.4867$ cm with errors in this value ranging from ± 0.005 cm ($\pm 0.14\%$ error), curves e and e'
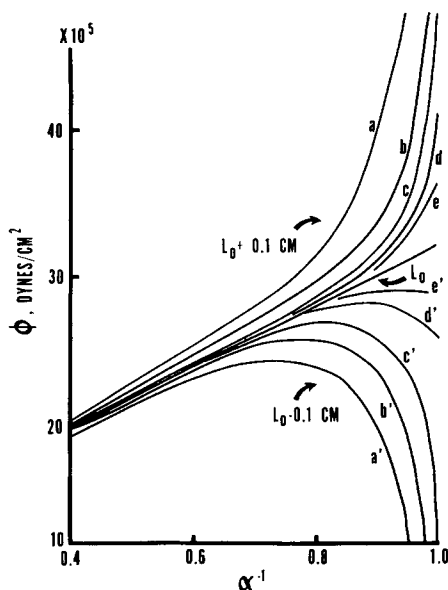

Fig. 4. Effect of error in estimating L_0 on the ϕ vs. α^{-1} plot. Errors in $L_0 = 3.4867$ cm are: ± 0.1 cm $a(+)$, $a'(-)$; ± 0.05 cm b,b'; ± 0.02 cm c, c'; ± 0.01 cm d,d'; ± 0.005 cm e,e'.

to ± 0.1 cm ($\pm 2.9\%$ error), curves a (+ error) and a' (− error). Curves b and b' were established similarly with errors in L_0 of ± 0.05 cm, while curves c and c', d and d' were obtained using errors of ± 0.02 cm and ± 0.01 cm, respectively. It is obvious from the figure that errors made in estimating L_0 could lead to significant errors in ϕ and, as a result, cause the ϕ-versus-α^{-1} plot to depart from linearity, especially in the region where $\alpha^{-1} > 0.7$. Small errors in estimating L_0 of the order of $\pm 0.1\%$ to $\pm 0.2\%$ seem to introduce little error in ϕ and leave the shape of the curve in the region below $\alpha^{-1} < 0.8$ and also the intercept C_1 essentially unchanged. However, large errors in L_0 of the order of $\pm 0.5\%$ to $\pm 3.0\%$ modify considerably the shape of the curve, especially in the region where $\alpha^{-1} > 0.7$, and lead to a significant error in estimating C_2 and C_1.

Stress-Strain in Swollen NBR Vulcanizates

S/S measurements were made on the NBR vulcanizates swollen in the solvent benzene. Swelling to the desired degree was made directly in the swelling cell. (To establish equilibrium conditions in the swollen rubber system, especially during partial swelling, it was necessary to leave the sample in the benzene-saturated atmosphere overnight in the tightly sealed glass swelling cell.) The volume fraction of rubber in the swollen sample, v_r was established as described earlier from eq. (4).

Typical stress-strain behavior in partially or completely swollen NBR vulcanizates is shown in Figure 5. C_2 is seen to decrease with swelling and approaches zero when the NBR vulcanizates are completely swollen. This behavior is also typical of other network systems.[5] For a completely swollen vulcanizate, the term $C_2\alpha^{-1}$ in eq. (2), becomes zero, and the equation reduces to

$$C_1 = fv_r^{1/3}(\alpha - \alpha^{-2})^{-1}/2A_0$$

which is identical to eq. (1), the simple equation of RET, when eq. (1) is corrected for network swelling.

Swelling Equilibrium Results

In the swelling equilibrium state, the free energy of mixing a polymeric network in a solvent is equivalent to the elastic free energy consequential to the network expansion. If the elastic free energy is computed from the simple statistical rubber elasticity theory expression, then a relationship, as shown by Flory and Rehner,[6] exists between the volume fraction of rubber in the swollen network at equilibrium, v_r, and the molecular weight between the crosslinks, M_c:

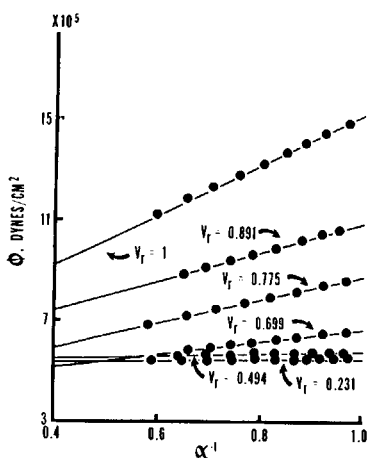$$-\ln(1 - v_r) - v_r - \chi v_r^2 = \rho V_0 M_c^{-1} v_r^{1/3} \qquad (5)$$

Fig. 5. Stress-strain at various degrees of swelling $(1/v_r)$ in NBR-peroxide vulcanizates.

which was later modified by Flory[7] to

$$-\ln (1 - v_r) - v_r - \chi v_r{}^2 = \rho V_0 M_c{}^{-1}(v_r{}^{1/3} - v_{r/2}).\qquad(6)$$

The terms on the left-hand sides of eqs. (5) and (6) represent the free energy of mixing, while those on the right represent the elastic retraction energy of the network.   Hence, the value of M_c can be determined from swelling equilibrium measurements if χ for the polymer–solvent system is known. In the present investigation, χ values for NBR in various solvents were established using M_c determined from stress–strain measurements made on swollen networks and v_r obtained from swelling equilibrium measurements. The v_r value was determined by swelling the sample in the solvent for 72 hr and changing the solvent every 24 hr.   No change in v_r was noticed on extended swelling of the samples beyond this period.   All v_r values were corrected when necessary for the soluble noncrosslinked polymer which was collected and dried in a vacuum oven at 80°C to constant weight.   Typical χ values for the NBR–benzene, NBR–cyclohexane, and NBR–n-heptane systems obtained according to eq. (6) are tabulated in Table II.   The χ

TABLE II
Chi Values for NBR–Benzene, NBR–Cyclohexane, and NBR–n-Heptane[a]

	χ Values		
Cure system	Benzene	Cyclohexane	N-Heptane
Sulfur–Altax	0.496	1.327	2.145
Sulfur–Santocure	0.492	1.347	2.110
Sulfur–Methyltuads	0.493	1.346	2.133
Methyltuads	0.497	1.328	2.101
Peroxides	0.488	1.348	2.131
Average	0.494	1.338	2.124

[a] All measurements made at 25°C.

value is much smaller in the better solvent benzene than in the other two solvents.   For the present NBR–solvent systems examined, χ was found to show very little dependence on v_r, thus allowing for the use of the average χ values shown in Table II to characterize NBR networks from the simple swelling equilibrium measurements which were made for the present NBR series in benzene at 25°C.

Effect of Cure Condition on NBR Crosslink Density

Figure 6 shows a plot of v_r versus cure time for peroxide vulcanizates cured at 158°C with 1, 2, and 4 phr dicumyl peroxide.   Crosslink density $\nu/2$, in crosslinks/cc, calculated through eq. (6) using the χ value of NBR–benzene shown in Table II, is plotted versus cure time for the same systems in Figure 7.   Both v_r and $\nu/2$ increase with an increase in cure agent concentration and with an increase in cure time, levelling off after 30 to 40 min of curing.   The various NBR vulcanizates shown in Figure 8 show the

same trend, although the rate of change in $\nu/2$ with cure time is noticed to differ from one cure system to another. At the cure agent levels shown in Figure 8, peroxide gives the highest degree of crosslinking in the series. Sulfur-cured NBR vulcanizates prepared using benzothiazole-type accelerator, such as benzothiazyl disulfide and N-cyclohexyl-2-benzothiazole-sulfenamide, show a delayed crosslinking reaction which is characteristic of
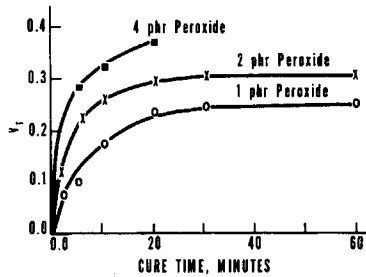

Fig. 6. Effect of cure time on the volume fraction of rubber in the swollen sample (v_r) in NBR–peroxide vulcanizates.
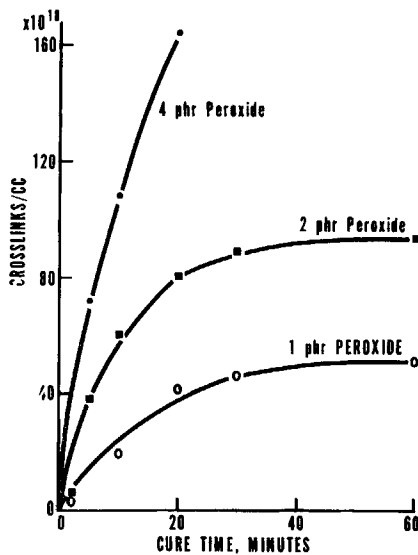

Fig. 7. Crosslink density (crosslinks/cc) vs. cure time in NBR–peroxide vulcanizates.

these accelerators. On the other hand, use of tetramethylthiuram disulfide with sulfur in the NBR formulation results in a fast-reacting system with a high degree of crosslinking. Tetramethylthiuram disulfide used as crosslinking agent without sulfur in the NBR formula yields a slow-reacting system with a constant crosslinking rate. Furthermore, the tetramethylthiuram disulfide–NBR vulcanizates show the least crosslink density for the cure systems shown in Figure 8.

The effect of crosslinking agent concentration on $\nu/2$ for the various NBR vulcanizates examined is shown in Figure 9. Since for the present NBR cure system examined, the crosslinking rates are time dependent, all
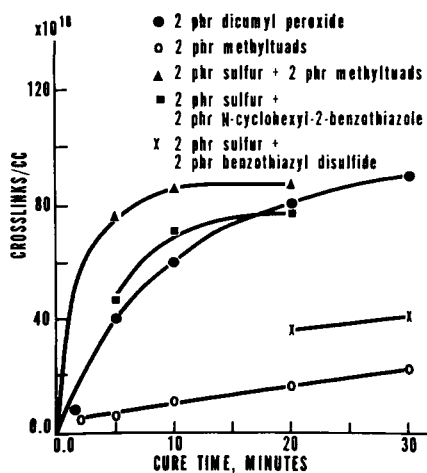

Fig. 8. Crosslink density vs. cure time in the various NBR's examined.
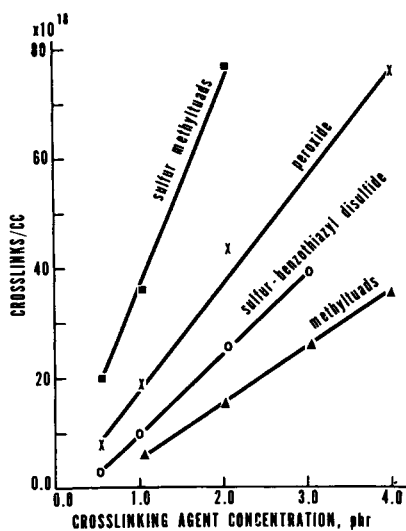

Fig. 9. Effect of crosslinking agent concentration on crosslink density in NBR vulcanizates cured for 40 min.

that we can say here about them is that the degree of crosslinking seems to increase linearly with cure agent concentration. Crosslink density was also found to increase with temperature.

TABLE III
M_c, v_r, $v/2$, and Crosslinking Efficiency in NBR Vulcanizates

Cure agent	Cure coagent	Cure time, min	Concentration, phr		v_r	M_c (physical)	$v/2$ (physical), moles/g $\times 10^{-4}$	Efficiency (physical), %[a]
			Agent	Coagent				
Dicumyl peroxide	none	20	1	none	0.2348	7,080	7.0	189
	none	20	2	none	0.2929	3,710	13.3	180
	none	20	4	none	0.3703	1,800	27.5	186
	none	60	1	none	0.2514	5,820	8.5	226
	none	60	2	none	0.3087	3,140	15.7	212
Sulfur	Altax	20	2	2	0.2356	8,380	6.2	80
	Altax	20	2	3	0.2408	7,840	6.7	86
	Altax	60	2	2	0.2568	6,460	8.0	102
Sulfur	Santocure	20	2	1	0.2771	4,860	9.0	115
	Santocure	20	2	2	0.2960	4,000	13.0	167
	Santocure	30	2	1	0.2784	4,800	9.2	117
Sulfur	Methyltuads	20	2	1	0.2742	4,700	10.9	140
	Methyltuads	20	2	2	0.3027	3,540	14.8	189
	Methyltuads	30	2	1	0.2933	3,840	13.3	171
Methyltuads	none	20	2	none	0.1750	20,400	2.5	30
	none	20	3	none	0.2119	11,600	4.5	36
	none	20	4	none	0.2329	8,700	5.9	35
	none	30	2	none	0.2003	13,700	3.8	46

[a] Moles crosslinks/moles cure agent.

Crosslinking Efficiency in NBR Vulcanizates

Table III shows a summary of v_r, M_c (physical), $v/2$ (physical), and the corresponding per cent crosslinking efficiency (physical) for the various NBR vulcanizates examined. (For explanation of these terms see ref. 8.) Per cent crosslinking efficiency was calculated as per cent (moles of crosslinks produced per gram rubber/mole of crosslinking agent used in the formula per gram rubber). The number of moles of crosslinks per gram rubber, which is equal to $v/2\rho N$, was computed from the measured quantities $v/2$ and ρ. M_c (physical) and $v/2$ (physical) were determined from the swelling equilibrium measurements through the use of eq. (6) and are not corrected for the chain entanglements and chain ends effects.[8–10] The corrections were not made because, owing to partial gelation of the polymer in solution during molecular weight determination, no reliable M_n value could be determined for the present NBR polymer. These corrections for chain ends and chain entanglements should lead to a decrease in M_c and to an increase in $v/2$ values and consequently should increase the per cent crosslinking efficiencies shown in Table III.

As shown in Table III, the per cent crosslinking efficiency (physical) in NBR vulcanizates depends on the nature of the crosslinking agent employed and on the cure time. Crosslinking efficiency is noticed to be independent of cure agent concentration when peroxide and Methyltuads, which have a first-order decomposition reaction, are the crosslinking agents. The crosslinking efficiency in the NBR–sulfur vulcanizate, however, is very much dependent on the concentration as well as the nature of the coagent used. (In calculating crosslinking efficiency for the NBR sulfur vulcanizates, sulfur is considered as the crosslinking agent and to have an S_8 ring structure.) Use of the coagent Methyltuads gives a high crosslinking efficiency (range 1.4 to 1.9 crosslinks/molecule S_8) and fast-reacting system, while use of the coagents Santocure and Altax results respectively in an efficient system (range 1.1 to 1.7 crosslinks/molecule S_8) with a moderate reaction rate and in a low-efficiency (range 0.8 to 1.0 crosslink/molecule S_8), slow-reacting system. The latter two systems show a delayed vulcanization reaction of $\sim$5 min with Santocure, 1 phr or less, and of $\sim$15 min with Altax. This is characteristic with thiazole and other scorch-delay accelerators and was recently explained in terms of their vulcanization reaction mechanisms.[11,12] The large differences observed in crosslinking efficiencies of NBR–Methyltuads with and without sulfur (see Table III) provide experimental support for the proposal in the literature that the reaction mechanisms for these two systems are quite different.

Maximum crosslinking efficiencies established for the various NBR vulcanizates investigated range from $\sim$225% for NBR–peroxide vulcanizates to $\sim$45% in the NBR–Methyltuads vulcanizates. Crosslinking efficiency of NBR–sulfur vulcanizates falls within this range and varies with the accelerator used: $\sim$190% with Methyltuads, $\sim$170% with Santocure, and 100% with Altax. These crosslinking efficiencies should increase as

mentioned earlier when the crosslinking efficiency is corrected for chain entanglements and chain ends effects.

References

1. A. Ciferri, *J. Polym. Sci.*, **54**, 149 (1961).

2. M. Mooney, J. Appl. Phys., **11**, 582 (1940).

3. R. S. Rivlin and D. W. Saunders, *Phil. Trans. Roy. Soc., London, A*, **243**, 251 (1951).

4. A. M. Hassan and L. N. Ray, Jr., *J. Appl. Polym. Sci.*, **15**, 145 (1971).

5. S. M. Gumbrell, L. Mullins, and R. S. Rivlin, *Trans. Faraday Soc.*, **49**, 1945 (1953).

6. P. J. Flory and J. Rehner, *J. Chem. Phys.*, **11**, 521 (1943).

7. P. J. Flory, *J. Chem. Phys.*, **18**, 108 (1950).

8. L. Mullins, *J. Appl. Polym. Sci.*, **2**, 1 (1959).

9. P. J. Flory, *Principles of Polymer Chemistry*, Cornell University Press, Ithaca, 1953.

10. F. Bueche, *Physical Properties of Polymers*, Interscience, New York, 1962

11. R. H. Campbell and R. W. Wise, *Rubber Chem. Tech.*, **37**, 635 (1964).

12. A. Y. Coran, *Rubber Chem. Tech.*, **37**, 673 (1964).